



# Application of Water Quality Index and Multivariate Statistical Analysis for Assessing Coastal Water Quality

Pintu Prusty<sup>1</sup> · Syed Hilal Farooq<sup>1</sup>

Received: 1 April 2020 / Accepted: 14 July 2020 / Published online: 24 July 2020  
© Springer Nature Switzerland AG 2020

## Abstract

Contamination of coastal water by seawater is a global phenomenon, which deteriorates the water quality. The present study aims to assess the suitability of coastal water for drinking and irrigation purposes with regard to seawater contamination. Conventional hydrochemical data have been utilized in conjunction with mathematical and statistical methods. Sixty groundwater and nine surface water samples were collected from the eastern coastal plains of Odisha, India and were analyzed for various physico-chemical parameters. A significant influence of seawater on water quality has been observed. Additionally, ion-exchange process has been identified to play a vital role in controlling the water chemistry. Application of hierarchical cluster analysis on water quality data produces two clusters of samples (C-1 and C-2) that are well-explained by the factors of principal component analysis. Higher dissolved salt contents in a majority of samples in the C-1 cluster have resulted in higher water quality indices that make them unsuitable for drinking purposes. Further, their placement in the Wilcox and USSLS diagrams indicated that these samples are even unsuitable for irrigation purposes. The C-2 cluster comprises 38% of water samples, which can be utilized for both drinking and irrigation purposes. The spatial distribution of water quality shows that the drinkable and irrigational water is mainly confined to a few patches in the area. These patches may be utilized for supplying the drinking water to the coastal population.

**Keywords** Water quality · Geochemical processes · Hierarchical cluster analysis · Principal component analysis · Coastal Odisha

---

✉ Syed Hilal Farooq  
hilalfarooq@iitbbs.ac.in

<sup>1</sup> School of Earth, Ocean, and Climate Sciences, Indian Institute of Technology Bhubaneswar, Argul Campus Odisha Khurda, India

## 1 Introduction

The coastal zones are some of the most densely populated areas across the globe. More than 40% of the global population lives within 100 km from the coast (Gopalakrishnan et al. 2019). The coastal areas are preferred residence and business destinations as they offer pleasant weather, rich mineral resources, ease of transportation, opportunities for maritime trade, and recreational or cultural activities (Neumann et al. 2015). However, the socio-economic development of the coastal region largely depends upon the quality and quantity of the available coastal water resources. The availability of substantial water supply and fertile soil in the area provide favorable conditions for the development of a wide variety of agricultural productivity (Nguyen et al. 2019). On the contrary, the deterioration of coastal water quality severely affects agricultural productivity, the aquatic environment, and human health (Milovanovic 2007). The surface water resources in many of the coastal regions are either quite limited, non-uniformly distributed, or biologically unfit for human consumption (Yidana and Yidana 2010). Further, studies have shown that the direct discharge of various toxic substances from domestic, agricultural, and industrial wastewater into the existing surface water bodies contaminates them substantially (Edokpayi et al. 2017). The surface water in coastal areas also faces severe salinity hazards due to the backwater of the sea (Vijay et al. 2011). Hence, there remains a minimal availability of good quality surface water in the coastal areas for human consumption. Under such conditions, the groundwater stands as the only source of good quality freshwater, and thus, it is extensively utilized for domestic, agriculture, and industrial purposes. Many fold increase in population and rapid industrialization in these regions have resulted in over-exploitation and unplanned utilization of groundwater resources (Adimalla 2019). This has caused not only a decrease in the fresh groundwater availability but also degradation of the groundwater quality in the coastal regions.

The quality of groundwater plays a vital role in deciding its usability for different purposes. Various geochemical processes, including the natural and anthropogenic activities, may affect the groundwater quality. The recharging water, while passing through various geological formations, may take up different heavy metals naturally (Mohankumar et al. 2016). Weathering and dissolution of rocks, leaching from the soil, and biological activities are some of the examples of natural processes that cause alterations in groundwater quality (Khatri and Tyagi 2015; Subba Rao et al. 2020). The anthropogenic factors responsible for the deterioration of the groundwater quality include improper waste disposal, mine discharges, percolation of agrochemicals, deforestation of woods, aquaculture, etc. (Hamed et al. 2018; Adimalla and Wu 2019). Further, the interaction of groundwater with the contaminated surface water can also pose a risk to the groundwater resources (Brindha et al. 2014). In coastal regions, seawater intrusion, caused primarily by over-exploitation of groundwater, is a major cause of concern that salinizes the groundwater resources (Alfarrah and Walraevens 2018). Additionally, flooding of coastal areas due to tidal activities, sea-level rise, and cyclones also degrade the coastal groundwater quality to some extent (Rezaie et al. 2019; Mohanty and Rao 2019).

The quality of coastal water resources varies widely over space and time; thus, a well-planned, comprehensive, and periodic monitoring is essential. Many of the coastal regions in south Asian countries, including Bangladesh, China, India, Malaysia, and Vietnam are facing substantial water shortage due to a rapid increase in the population (Kura et al. 2013; Mahmuduzzaman et al. 2014; Krishnakumar et al. 2014; Minderhoud et al. 2017; Wang et al. 2018). In India, the scarcity of fresh groundwater is alarming, especially in the eastern coastal regions due to the higher influence of seawater (Mukhopadhyay and Karisiddaiah

2014; Prusty and Farooq 2020). An earlier study in the Puri district of eastern India has demonstrated that anthropogenic activities such as domestic waste disposal, effluents from septic tanks, soak pits, pit latrines, and leakage of drains are the main causes of groundwater quality degradation (Vijay et al. 2011). Further, studies based on statistical analysis have identified that the variable seawater-groundwater mixing is responsible for the saline nature of groundwater in the area (Mohapatra et al. 2011; Prusty et al. 2018). In a recent study, the quantity of seawater-freshwater mixing in the area has been calculated (Mohanty and Rao 2019). However, limited attempts have been made to link the effect of seawater on coastal groundwater resources with their suitability for various utilization purposes. Further, a detailed assessment of the surface water quality for irrigation usage in the coastal region has not been done. These are the vital research gaps that need to be filled for a better understanding, planning, and judicious utilization of coastal groundwater resources. To fill these gaps in scientific knowledge, the present study has been conducted with the aims to (i) assess the surface water and groundwater quality, and (ii) evaluate their suitability for drinking and irrigation purposes in the coastal region of Puri district of India. Multivariate statistical analysis has been applied to the hydrochemical data, and water quality indices were calculated to understand the prevailing geochemical processes and evaluate their impact on the coastal water quality. Geospatial analysis has also been adopted to identify the regions with potential drinking and irrigation water resources.

## 2 Materials and Methods

### 2.1 Site Description

The study area is located in the Puri district of Odisha, which lies along the East coast of India between 19°40′-20°10′ N latitudes and 85°25′-86°25′ E longitudes. The coastal district has a population of 1.6 million and an area of around 3479 sq. km (Census of India 2011). The population density of the area is 488 persons per km<sup>2</sup>, which is quite high as compared to other coastal regions. The district falls in the Mahanadi river basin and consists of varied rock formations of Archean to Recent (Quaternary) age. The Tertiary and Quaternary formations cover the major parts of the district, while the basement rocks of Archean age are found in the hilly regions (Central Ground Water Board 2013). The Archean rocks comprise granite gneisses and charnockites with some isolated patches of khondalites. The coastal plains are covered by the porous-medium unconsolidated formations of Tertiary and Quaternary age. In the Tertiary formations, groundwater occurs under a phreatic condition at a shallow surface and semiconfined conditions at greater depth. The exploratory boreholes drilled across the coastal tracks of the state show the presence of different hydrological zones such as freshwater, freshwater underlain by saline water, freshwater overlain by saline water, and alternate fresh-saline water zones (Fig. 1a; Central Ground Water Board 2013). The study area has a very dense network of rivers, including Devi, Kushabhadra, Bhargabi, Prachi, Kadua, Ratnachira, and Dhanua, which fall into the Bay of Bengal. These rain-fed rivers show varied drainage characteristics in-line with the seasonal changes in rainfall. They usually occur at a higher level from the groundwater table during summer and nearer to the groundwater table during monsoon season (Central Ground Water Board 2013). A warm and humid climate prevails in the region with an average annual rainfall of 1450 mm during June-October from the south-west monsoon (Patra et al. 2012).

## 2.2 Sample Collection and Analytical Methods

Sixty-nine water samples, including sixty groundwater (labeled as 1–60) and nine surface water (labeled as R1-R9), were collected from the coastal tract of Puri district, Odisha. The groundwater samples were collected from actively used tube wells having an average depth of 13–15 m. These tube wells were pumped for 3–5 min to clear the casing water before the collection of water samples. Surface water samples from a certain depth (~1 m from water surface) were collected from all the rivers flowing in the coastal plain. These water samples were collected in pre-cleaned polyethylene bottles of 250 mL capacity during June 2017. The sample locations were geo-referenced using a Global Positioning System (Trimble, Juno S-3

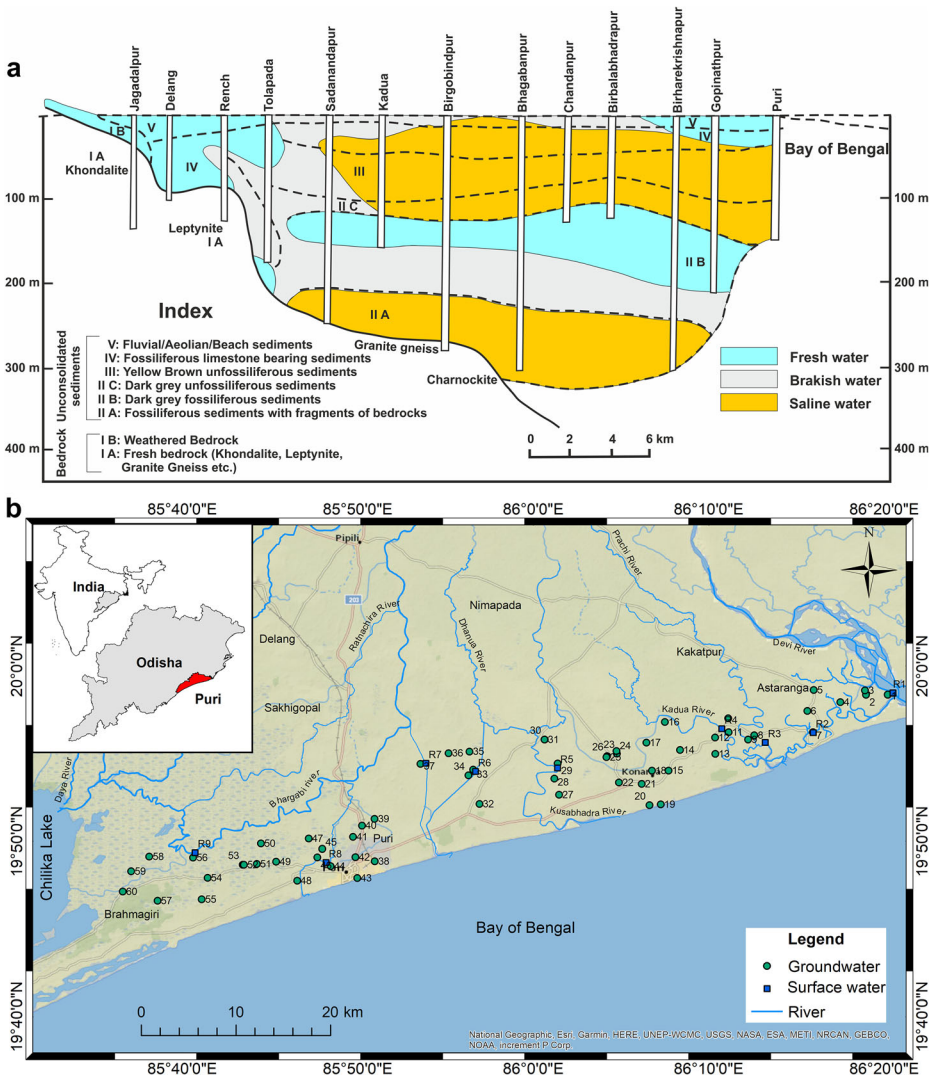


**Fig. 1** Location map of study area. **(a)** Hydrogeological profile of study area (modified after Central Ground Water Board 2014), and **(b)** Sample collection sites

model), and they lie within 10 km from the coastline (Fig. 1b). Two filtered samples (0.45  $\mu\text{m}$  polycarbonate membrane filter) were collected from each location: (i) non-acidified for analysis of anions and (ii) acidified with ultrapure  $\text{HNO}_3$  for analysis of cations. Temperature, pH, and electrical conductivity (EC) were measured *in situ* using a pre-calibrated portable Multi-Parameter system (Orion Star A329, Thermo Fisher Scientific) in combination with pH (ROSS ultra gel triode) and EC (4 cell graphite) electrodes. Total dissolved solids (TDS) content was calculated from the measured EC values using the expression,  $\text{TDS (mg/L)} = \text{EC } (\mu\text{S/cm}) \times 0.64$  (Lloyd and Heathcote 1985). The samples were stored at a lower temperature (4  $^\circ\text{C}$ ) in the laboratory to prevent any change in water chemistry caused by microbial activities. Fluoride ( $\text{F}^-$ ),  $\text{NO}_3^-$ , and major ion ( $\text{Cl}^-$ ,  $\text{SO}_4^{2-}$ ,  $\text{Ca}^{2+}$ ,  $\text{K}^+$ ,  $\text{Mg}^{2+}$ , and  $\text{Na}^+$ ) concentrations were measured by Ion Chromatography system (883 Basic IC Plus, Metrohm). Alkalinity ( $\text{CO}_3^{2-}$  and  $\text{HCO}_3^-$ ) was determined by Auto-titrator (848 Titrino plus, Metrohm) following standard titrimetric method (Rice et al. 2012). The accuracy of the hydrochemical data was checked by calculating the charge balance of individual samples, and the errors in the charge balance remained within the acceptable range of  $\pm 10\%$  (Adimalla and Wu 2019).

### 2.3 Multivariate Statistical Analysis

Multivariate statistical analysis is widely used in hydrological studies to understand the multi-dimensional problems. These studies generally deal with a large number of physico-chemical variables and observations. In the present study, the physico-chemical parameters analyzed in both groundwater and surface water samples were used collectively for hierarchical cluster analysis (HCA) and principal component analysis (PCA). The data sets were log-transformed to accommodate a wide range of parameters. HCA and PCA were performed on the log-transformed data using XLSTAT software (2016). HCA was implemented using Ward's linkage method with squared Euclidean distance as a measure of dissimilarity to classify the water samples. PCA was applied to find out the relationships between the physico-chemical parameters and the sample locations. The statistical significance of PCA was tested by Kaiser–Meyer–Olkin (KMO) and Bartlett's tests. Further, the varimax rotation technique was implemented for the maximum participation of the variables (Matiatos et al. 2014). The parameters and the sample locations were correlated by the principal components (PCs) in terms of factor loadings and factor scores, respectively. Based on the Kaiser criterion, the PCs having eigenvalues  $\geq 1$ , are retained (Kaiser 1974).

### 2.4 Water Quality Index Calculation

The quality of drinking water can be evaluated by using the water quality index (WQI) method (Horton 1965). The WQI provides the overall water quality by combining the effects of individual water quality parameters in comparison to standard prescribed limits. In the present study, the World Health Organization (WHO 2011) standard limits prescribed for the drinking water have been used to calculate the WQI values for the individual water samples. The concentration of  $\text{K}^+$  was not included in this calculation as it has no WHO prescribed limit. WQI calculation involves four steps. In the first step, a weight is assigned to each of the water quality parameters based on their relative effects on water quality. The parameters such as  $\text{Cl}^-$ ,  $\text{F}^-$ ,  $\text{NO}_3^-$ ,  $\text{SO}_4^{2-}$ , and TDS are assigned with the highest weight of 5 due to their higher impact on overall water quality (Krishnakumar et al. 2014). Alkalinity and pH, which have a relatively minor role in water quality, are given a minimum weight of 1 (Kumar et al. 2014). The

remaining parameters are assigned a weight varying between 1 and 5. The second step involves the calculation of the relative weight of each parameter as the ratio of the assigned weight and total weight (Eq. 1). In the third step, a quality rating scale is computed for each parameter in each water sample. This is done by dividing the concentration of water quality parameters with their WHO prescribed limits and multiplication by 100 (Eq. 2). In the final step, the calculated relative weight and quality rating scale are multiplied to find out the water quality sub-index (Eq. 3), and the summation of all the water quality sub-index for each water quality parameter gives the WQI of the water sample (Eq. 4). The assigned weight, calculated relative weight, and WHO prescribed limit for the water quality parameters are presented in Table 1.

$$W_i = w_i / \sum_{i=1}^n w_i \quad (1)$$

$$q_i = \left( \frac{C_i}{S_i} \right) \times 100 \quad (2)$$

$$SI_i = W_i \times q_i \quad (3)$$

$$WQI = \sum_{i=1}^n SI_i \quad (4)$$

where  $i$  stands for water quality parameter,  $W_i$  for relative weight,  $w_i$  for assigned weight,  $n$  for the number of parameters,  $q_i$  for quality rating scale,  $C_i$  for measured concentration,  $S_i$  for WHO prescribed drinking limit, and  $SI_i$  for water quality sub-index. For the calculation of WQI, the concentrations of water quality parameters in mg/L have been utilized.

**Table 1** Assigned weight ( $w_i$ ) and relative weight ( $W_i$ ) of water quality parameters with their WHO (2011) permissible limits

Water quality parameters	WHO permissible limit <sup>a</sup>	$w_i$	$W_i$
pH	7.5 <sup>b</sup>	1	0.03
TDS	1000	5	0.14
Na <sup>+</sup>	200	4	0.11
Ca <sup>2+</sup>	200	3	0.08
Mg <sup>2+</sup>	150	3	0.08
Cl <sup>-</sup>	250	5	0.14
SO <sub>4</sub> <sup>2-</sup>	500	5	0.14
Alkalinity	600	1	0.03
F <sup>-</sup>	1.5	5	0.14
NO <sub>3</sub> <sup>-</sup>	50	5	0.14
Sum		37	1

<sup>a</sup> pH is in numerical value, EC is in  $\mu\text{S}/\text{cm}$ , all others are in mg/L; <sup>b</sup> Average of lower and upper WHO permissible limits

### 3 Results and Discussion

#### 3.1 Hydrogeochemistry

The summary of the measured physico-chemical parameters in the collected groundwater and surface water samples, along with the respective WHO permissible limits are presented in Table 2. The groundwater shows moderately acidic to mildly alkaline characteristics, while the surface water has alkaline nature. Except for three groundwater and two surface water samples, the pH values of the remaining water samples are within the WHO (2011) prescribed permissible limit for drinking water (6.5–8.5). However, the pH values in those three groundwater and two surface water samples are lower and higher than the WHO permissible limit, respectively. The EC values reflect the dissolved salt contents or salinity of water, and its higher values are generally indicative of higher major ion concentrations in the water (Prasanth et al. 2012). The EC values ranged from 40.5 to 25,170  $\mu\text{S}/\text{cm}$  in groundwater and 207.6–52760  $\mu\text{S}/\text{cm}$  in surface water (Table 2). The extremely higher EC values of the surface water are equivalent to the EC values of the seawater.

The concentration and composition of various dissolved constituents determine the quality of water and its suitability for various purposes. The major ions show wide variations in their concentrations in both groundwater and surface water samples (Table 2). In these samples,  $\text{Na}^+$  and  $\text{Cl}^-$  are found as the dominating cation and anion species, respectively. The concentration of  $\text{Na}^+$  varies from 3.8 to 5274 mg/L in groundwater and 3–11885 mg/L in surface water. Chloride has the highest ionic concentration among all the ions, and its concentration ranges from 4.2 to 7381 mg/L in groundwater and 7.2–20688 mg/L in surface water. Both the groundwater and surface water show enormously higher concentrations of  $\text{Na}^+$  and  $\text{Cl}^-$ , indicating that the water quality in the area is most likely affected by the seawater. The concentration of  $\text{K}^+$  shows the least variation with the range of 0.2–171.1 mg/L in groundwater and 2.3–397.2 mg/L in surface water. In groundwater,  $\text{Ca}^{2+}$  and  $\text{Mg}^{2+}$  concentrations range between 1.4 and 322.4 mg/L and 1.3–518.9 mg/L, respectively. Similarly, the concentrations of  $\text{SO}_4^{2-}$  and alkalinity vary from 0.03 to 1254 mg/L and 6.1–835.7 mg/L, respectively. In

**Table 2** Summary of water quality parameters in groundwater (n = 60) and surface water (n = 9)

Parameters	Groundwater			Surface water			WHO (2011) permissible limits
	Mean	Min	Max	Mean	Min	Max	
pH	7.2	5.4	8.4	8.0	7.0	8.7	6.5–8.5
EC	3260.4	40.5	25,170	24,805	207.6	52,760	-
TDS	2086.7	25.9	16,109	15,875	132.9	33,766	1000
Alkalinity	251.8	6.1	835.7	119.2	69.9	252.2	600
$\text{Cl}^-$	690.4	4.2	7381.3	9643.3	7.2	20,688	250
$\text{SO}_4^{2-}$	102.4	0	1253.7	1172.7	6.6	2538.8	500
$\text{Na}^+$	468.6	3.8	5273.8	5539.5	3	11,885	200
$\text{K}^+$	28	0.2	171.1	187.6	2.3	397.2	-
$\text{Ca}^{2+}$	55.2	1.4	322.4	235.6	19.7	475.2	200
$\text{Mg}^{2+}$	50.8	1.3	518.9	665.9	6.5	1430.2	150
$\text{F}^-$	0.62	0.01	2.6	0.51	0.3	0.7	1.5
$\text{NO}_3^-$	12.6	0.4	289.3	4.8	0.2	22.4	50

pH is in numerical value, EC is in  $\mu\text{S}/\text{cm}$ , all others are in mg/L



surface water,  $\text{Ca}^{2+}$  ranges from 19.7 to 475.2 mg/L,  $\text{Mg}^{2+}$  from 6.5 to 1430 mg/L,  $\text{SO}_4^{2-}$  from 6.6 to 2539 mg/L, and alkalinity from 69.9 to 252.2 mg/L. The dominance of  $\text{Mg}^{2+}$  over  $\text{Ca}^{2+}$  concentrations in the coastal water further suggests the influence of seawater on groundwater chemistry. By comparing these concentrations with the WHO permissible limit, it is observed that the deviation from the permissible limit is more prominent in the surface water than the groundwater. The rivers falling in the Bay of Bengal have long course, and their flow becomes sluggish in the coastal plain due to huge sediment transport (Barik et al. 2019). It not only allows significant evaporation but also facilitates the easy inflow of seawater in the upstream direction due to periodic sea-level changes in response to the tidal activities (Central Ground Water Board 2013).

Although fluoride is an essential element in drinking water, its higher concentration is considered as a contaminant (Adimalla 2020). Relatively higher  $\text{F}^-$  concentrations were observed in the groundwater (0.01–2.6 mg/L) than the surface water (0.3–0.7 mg/L). Six out of sixty groundwater samples have  $\text{F}^-$  concentrations higher than the WHO (2011) permissible limit (1.5 mg/L), while it remained within the permitted limit in all the surface water samples. These six groundwater samples also show higher  $\text{Cl}^-$  concentrations. The association of  $\text{F}^-$  with  $\text{Cl}^-$  indicates its seawater origin and negates the possible influx from the fertilizers used in the agriculture fields in nearby areas. However, the average concentration of  $\text{F}^-$  in groundwater remains 0.62 mg/L, which is within the WHO permissible limit. The concentration of  $\text{NO}_3^-$  is usually used as an indicator of anthropogenic influence on water quality. Except for four groundwater samples,  $\text{NO}_3^-$  concentrations in the remaining water samples are found to be well within the WHO (2011) prescribed limit (50 mg/L), indicating no significant influence of anthropogenic activities in the study area. Out of those four groundwater samples, three samples have slightly higher  $\text{NO}_3^-$  concentrations (64–86 mg/L), and one sample has an extremely high concentration (289 mg/L). The locations of these samples are found to be closer to the sewage system and sanitation sites.

### 3.2 Multivariate Statistical Analysis

Based on the chemical characteristics, the water samples were grouped into two clusters by HCA (Fig. 2). Cluster 1 (C-1) includes 43 samples (36 groundwater and 7 surface water), which have higher dissolved constituents (average TDS of 3231 mg/L in groundwater and 20,360 mg/L in surface water). The remaining 26 samples, including two surface water, have lesser dissolved content (average TDS of 370 mg/L in groundwater and 175 mg/L in surface water) and are combined in cluster 2 (C-2). The variation of water quality parameters in these two clusters of samples is presented in the Schoeller plot (Fig. 3). The C-1 samples have higher values of all water quality parameters, while the C-2 samples have lower values. The concentrations of  $\text{SO}_4^{2-}$  are found to be much lower ( $< 1$  mg/L) in seven of the groundwater samples in the C-1 cluster, which have higher alkalinity values (Fig. 3). This is attributed to  $\text{SO}_4^{2-}$  reduction process associated with the seawater interaction. The reduction of  $\text{SO}_4^{2-}$  by sulfate-reducing bacteria has been reported by earlier studies, which causes transformation of sulfate and organic matters to hydrogen sulfide (Rabus et al. 2013; Central Ground Water Board 2014). For both clusters of samples, the dominance of average cations are in the order of  $\text{Na}^+ > \text{Mg}^{2+} > \text{Ca}^{2+} > \text{K}^+$ . The average anion concentrations are in the order of  $\text{Cl}^- > \text{SO}_4^{2-} > \text{alkalinity} > \text{NO}_3^- > \text{F}^-$  in the C-1 samples and  $\text{Cl}^- > \text{alkalinity} > \text{SO}_4^{2-} > \text{NO}_3^- > \text{F}^-$  in the C-2 samples. However, the concentrations of the water quality parameters are much higher in the C-1 samples as compared to the C-2 samples (Fig. 3).



The KMO measure of sample adequacy (0.79) and the significance level of Bartlett's test of sphericity ( $< 0.0001$ ) suggest that PCA can be applied suitably on the data for extracting useful information (Kaiser 1974). Two PCs (PC-1 and PC-2) were extracted from PCA, which explained 74.4% of cumulative data variability. PC-1 explains the majority of data variance (56.4%), and PC-2 accounts for 18% of data variability. The distribution of factor scores (sample locations) and factor loadings (physico-chemical parameters) are presented in Fig. 4a, b. PC-1 has positive loadings of all water quality parameters, while PC-2 has negative loadings of  $\text{Ca}^{2+}$ ,  $\text{NO}_3^-$ ,  $\text{SO}_4^{2-}$ , and positive loadings of the remaining parameters (Fig. 4a). These two PCs can be positively related to the C-1 samples and negatively related to the C-2 samples (Fig. 4a, b). Strong positive loadings of  $\text{Cl}^-$ , EC, and other major ions in PC-1 indicate a strong influence of seawater on C-1 samples (Alfarrah and Walraevens 2018). On the contrary, lower values of PC-1 and PC-2 parameters in C-2 samples suggest a limited effect of seawater on water quality. Thus, from the concentrations of water quality parameters and their association with the sample clusters, it can be interpreted that the C-1 samples are characterized by high salinity and C-2 samples by low salinity.

### 3.3 Evolution of Coastal Water

The hydrochemical facies evolution (HFE) diagram proposed by Giménez-Forcada (2010) has been used to identify the geochemical processes controlling the coastal water quality. The HFE diagram explains the coastal hydrochemical processes viz. seawater-freshwater mixing and ion-exchange, and defines freshening/intrusion stages with respect to the composition of two end-members (i.e., freshwater and seawater). For the plotting of the HFE diagram, the seawater composition was taken from an earlier study (Prusty et al. 2020), and a theoretical freshwater composition was derived from the collected water samples (Giménez-Forcada 2014). It is

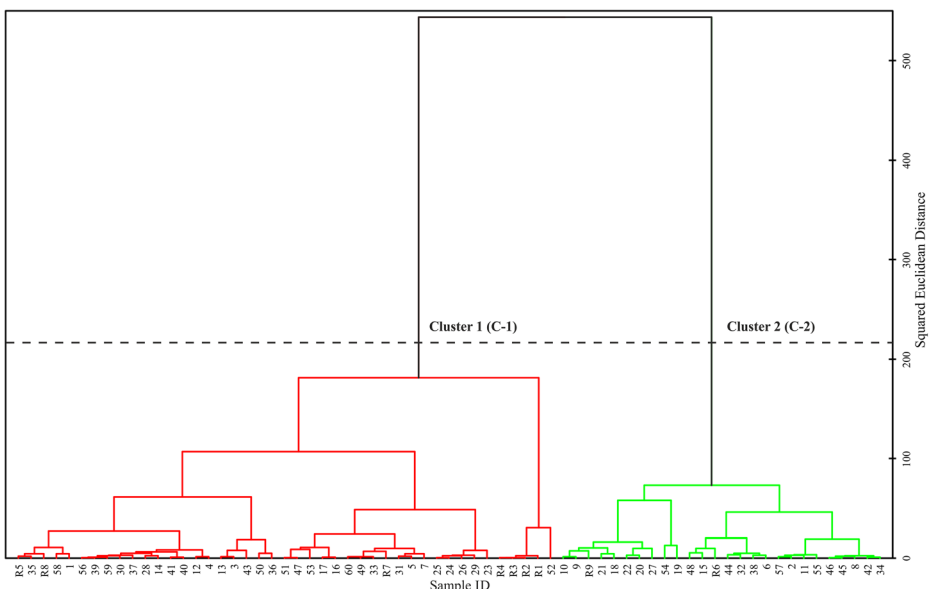
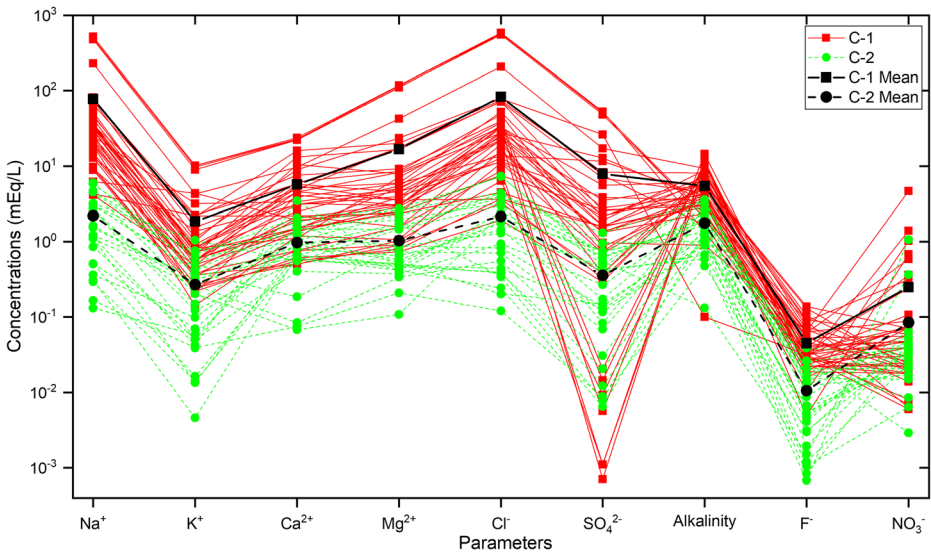
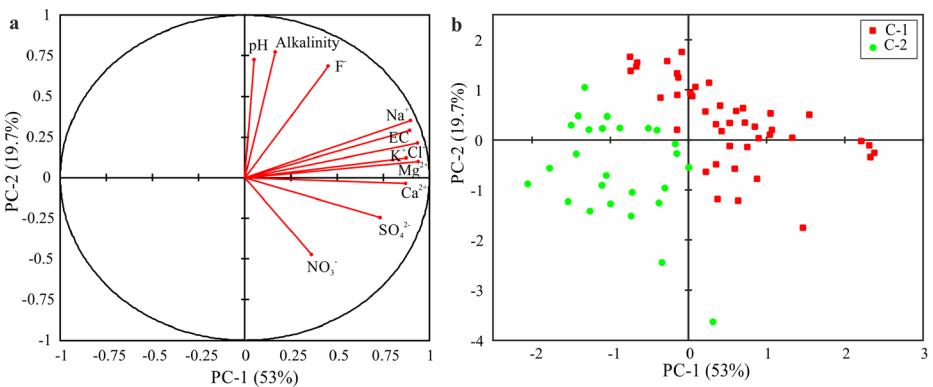


Fig. 2 Hierarchical cluster analysis showing clustering of the sample locations into C-1 and C-2 clusters



**Fig. 3** Schoeller plot showing variation of water quality parameters in two clusters of water samples

observed that  $\text{HCO}_3^-$  is dominant over  $\text{SO}_4^{2-}$  and  $\text{Ca}^{2+}$  over  $\text{Mg}^{2+}$  in all the samples with lower content ( $< 50\%$ ) of  $\text{Cl}^-$  and  $\text{Na}^+$ , respectively; therefore,  $\text{SO}_4^{2-}$  and  $\text{Mg}^{2+}$  ions are not shown in Fig. 5 (Giménez-Forcada and Sánchez San Román 2015). A majority of collected water samples (58% of groundwater and 78% of surface water) fall in field 4 (Na-Cl type) of the HFE diagram. It is observed that freshening (i.e., mixing of freshwater) is the dominant process in controlling the groundwater chemistry as 80% of the samples occur above and left of the mixing line (Fig. 5). Around 13% of the groundwater samples are found to be of Na- $\text{HCO}_3$  type (field 1). The water of this field evolves by freshening and simultaneous direct ion-exchange process (Giménez-Forcada 2010). The freshening causes enrichment of  $\text{Ca}^{2+}$  and  $\text{HCO}_3^-$  in the water; however, the direct ion-exchange process exchanges the  $\text{Ca}^{2+}$  of water with the  $\text{Na}^+$  of aquifer sediments. The combined process leads to the movement of Na-Cl water towards Na- $\text{HCO}_3$  water following the evolution path 4-3-2-1. Further, 10% of groundwater samples are MixCa- $\text{HCO}_3$  type (field 9), which is developed with the progression of the



**Fig. 4** Biplots of principal components explaining the relationship of (a) physico-chemical parameters and (b) sample locations

freshening process following the evolution path 1-5-9-13. The remaining 20% of the collected groundwater samples fall below and right of the mixing line and are in the intrusion stage (i.e., mixing of seawater; Fig. 5). In this process, the Ca-HCO<sub>3</sub> water moves towards the seawater composition (Na-Cl type) following the evolution path 13-14-15-16-12-8-4 (Giménez-Forcada 2010). In the initial stage of intrusion, reverse ion-exchange (vice-versa of direct ion-exchange) takes place between the water and aquifer sediment, and Ca-Cl water is developed through the evolution path (13-14-15-16). Placement of only one water sample in field 15 (Ca-MixCl water) indicates a limited role of reverse ion-exchange. The development of MixNa-Cl and Na-Cl water types indicates the final stage of the intrusion process. It is also observed that a few of the groundwater and all the surface water samples fall close to the mixing line (Fig. 5). These water samples are evolved through the binary mixing of the seawater and freshwater types without the intervention of the ion-exchange processes. The mixing of seawater in the surface water channels is attributed to the landward flow of seawater during high tide periods. In view of the cluster classes, it is observed that the C-1 samples are either in the final stage of intrusion or in the initial stage of freshening; thus, they are dominantly under the influence of seawater. However, the C-2 samples are mostly in the final stage of the freshening process with the development of Na-HCO<sub>3</sub> to MixCa-HCO<sub>3</sub> water types.

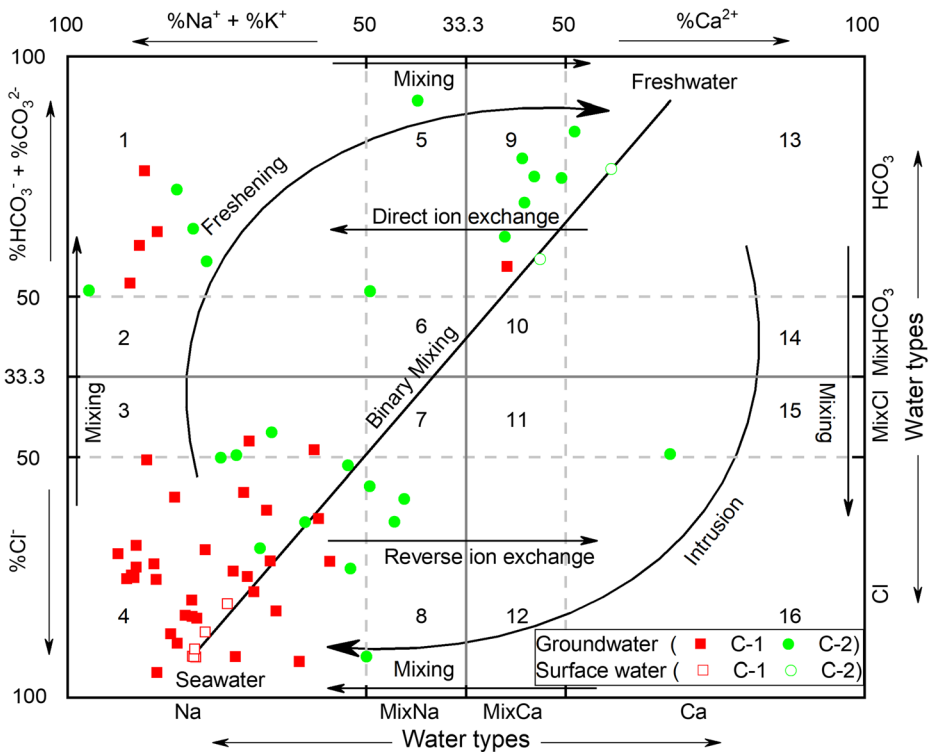


**Fig. 5** Identification of the geochemical processes controlling coastal water chemistry from the HFE diagram (1: Na-HCO<sub>3</sub>, 2: Na-MixHCO<sub>3</sub>, 3: Na-MixCl, 4: Na-Cl, 5: MixNa-HCO<sub>3</sub>, 6: MixNa-MixHCO<sub>3</sub>, 7: MixNa-MixCl, 8: MixNa-Cl, 9: MixCa-HCO<sub>3</sub>, 10: MixCa-MixHCO<sub>3</sub>, 11: MixCa-MixCl, 12: MixCa-Cl, 13: Ca-HCO<sub>3</sub>, 14: Ca-MixHCO<sub>3</sub>, 15: Ca-MixCl, 16: Ca-Cl)

Molar ionic ratios are further used for a clear understanding of the geochemical processes. In a hydrological system,  $\text{HCO}_3^-$  is a characteristic of freshwater, while  $\text{Cl}^-$  is indicative of seawater in the coastal areas (Kumar et al. 2014). In the present study, their ratio ( $\text{Cl}^-/\text{HCO}_3^-$ ) has been utilized to reaffirm the effect of seawater on the coastal water quality (Fig. 6). Studies have shown that  $\text{Cl}^-/\text{HCO}_3^-$  ratio higher than 0.5 in coastal water gives a clear indication of seawater influence in modulating the water chemistry (Najib et al. 2017). Around 53% of groundwater and eight surface water samples are found to be under the influence of seawater due to their higher  $\text{Cl}^-/\text{HCO}_3^-$  ratio ( $> 0.5$ ) and higher concentrations of  $\text{Cl}^-$  ( $> 250$  mg/L). Further, these samples belong to the C-1 cluster, which gives confirmative evidence of seawater influence on the samples grouped in the C-1 cluster (Fig. 6). The C-2 samples have less  $\text{Cl}^-$  concentration ( $< 250$  mg/L) that restricts the effect of seawater in the C-2 samples. The ionic ratio values also confirm the higher influence of seawater on the surface water samples since they have higher  $\text{Cl}^-$  concentrations as well as  $\text{Cl}^-/\text{HCO}_3^-$  ratios (Fig. 6). Therefore, there is a higher chance that the groundwater quality may degrade due to their recharge from the salinized surface water sources.

### 3.4 Water Quality for Drinking Purpose and Associated Health Issues

WQI is widely used to evaluate the water quality and determine its suitability for drinking purposes. Based on WQI values, water quality can be classified into different classes such as excellent ( $< 50$ ), good (50–100), poor (100–200), very poor (200–300), and unsuitable ( $> 300$ ) for drinking purpose (Sahu and Sikdar 2008). The classes of WQI for individual groundwater and surface water samples are shown in Fig. 7. The WQI values range from 5.6 to 970 in the groundwater and from 10.3 to 2391 in the surface water samples. Around 60% of the groundwater samples are found to be of good to excellent water type, 33% show poor to very poor water type, and the remaining (7%) are unsuitable for human consumption. Six out of nine surface water

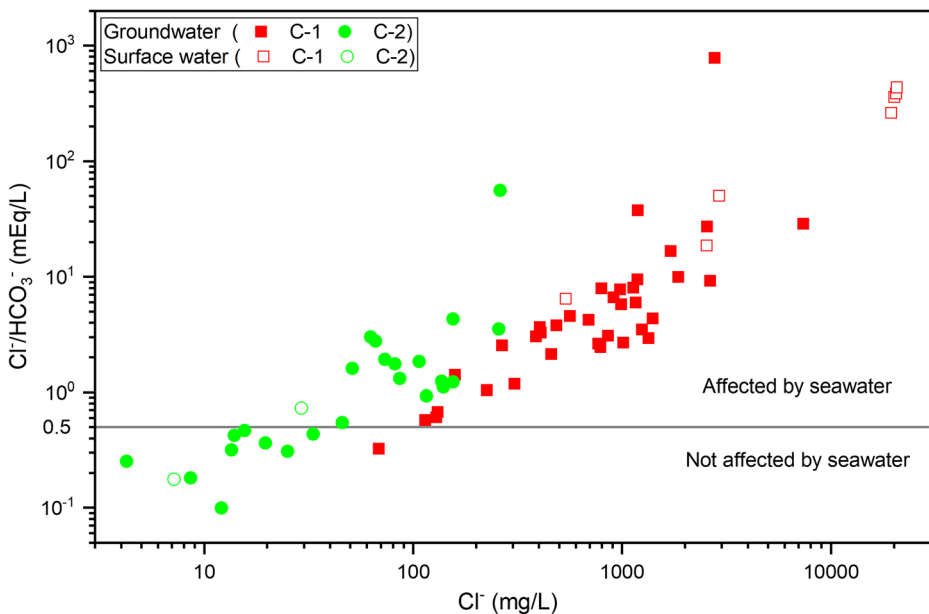


Fig. 6 Bivariate plot of  $\text{Cl}^-/\text{HCO}_3^-$  vs.  $\text{Cl}^-$  depicting the effect of seawater on coastal water

samples are also found to be unsuitable for drinking (WQI > 300), while the remaining three are excellent to good water types. These three surface water samples are confined to a small part of the study area and cannot fulfill the water demands of the study area. Thus, the local population mainly depends upon the groundwater resources to meet their daily water requirements. A majority of the C-1 samples (70%) fall in poor to unsuitable for drinking categories and cannot be utilized for drinking without prior treatment (Fig. 7). The C-2 samples comprise excellent water types and are safe for direct consumption with regard to the major ion concentrations.

Pearson’s correlation test was conducted for C-1 and C-2 clusters separately to understand the contribution of various physico-chemical parameters to WQI. For both clusters, WQI is found to be strongly related to TDS, Cl<sup>-</sup>, Na<sup>+</sup>, and Mg<sup>2+</sup> (Table 3). However, these parameters have a higher influence in the C-1 cluster as compared to the C-2 cluster with additional contributions from SO<sub>4</sub><sup>2-</sup> and Ca<sup>2+</sup>. Besides, the major ions (except alkalinity) show strong positive correlations among themselves in the C-1 cluster. Higher values of physico-chemical parameters and their strong positive correlations (TDS, Cl<sup>-</sup>, Na<sup>+</sup>, Mg<sup>2+</sup>, Ca<sup>2+</sup>, and SO<sub>4</sub><sup>2-</sup>) with WQI are indicative of seawater influence on the samples grouped in C-1 cluster. On the contrary, pH and alkalinity do not show a significant correlation either with WQI or with other parameters (Table 3); thus, they have a limited role in affecting the WQI values in the study area. Similarly, with regard to the NO<sub>3</sub><sup>-</sup> and F<sup>-</sup> contaminations, the water is safe as they do not show a significant correlation with WQI. The use of WQI for assessing the combined effects of major ions on water quality of coastal regions has been proved to be quite successful in many parts of the world (Kumar et al. 2014; Şener et al. 2017; Adimalla et al. 2018).

From the above discussion, it can be inferred that the groundwater samples grouped in the C-2 cluster are safe for drinking, while 40% of total groundwater and the surface water samples belonging to the C-1 cluster are not suitable for drinking usage on account of their higher dissolved salts contents. Therefore, the consumption of water samples grouped in the C-1 cluster could lead to several health issues. The long term intake of saline water causes higher Na<sup>+</sup> concentrations in the body, which reduces the kidney’s ability to remove water and results

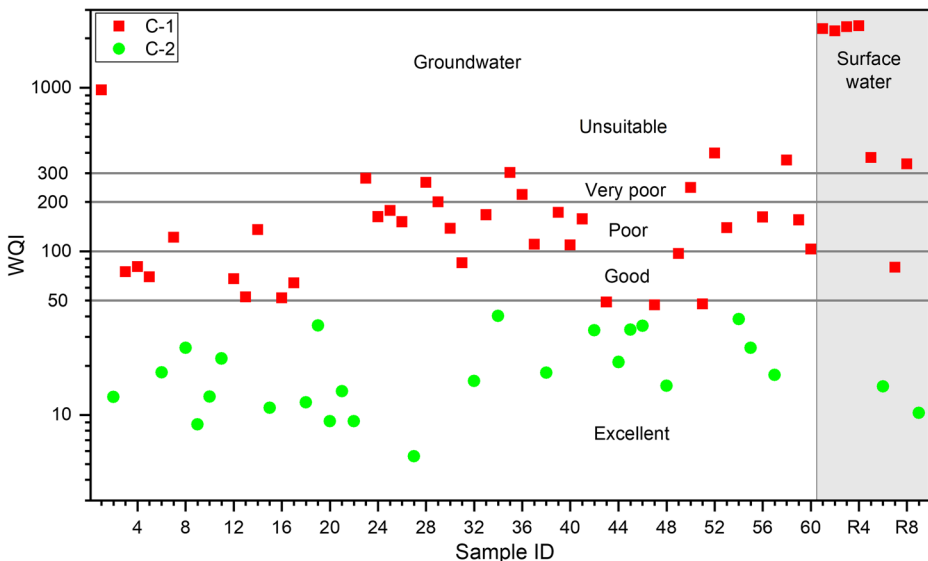


Fig. 7 Water quality indices (WQI) of individual groundwater and surface water samples

**Table 3** Pearson's correlation matrix showing relationships among water quality index (WQI) and physico-chemical parameters of water in the cluster classes

Cluster 1	WQI	pH	TDS	Alkalinity	Cl <sup>-</sup>	SO <sub>4</sub> <sup>2-</sup>	Na <sup>+</sup>	Ca <sup>2+</sup>	Mg <sup>2+</sup>	F <sup>-</sup>	NO <sub>3</sub> <sup>-</sup>
WQI	1										
pH	0.21	1									
TDS	<b>0.99</b>	0.20	1								
Alkalinity	-0.33	-0.06	-0.28	1							
Cl <sup>-</sup>	<b>1.00</b>	0.22	<b>0.98</b>	-0.34	1						
SO <sub>4</sub> <sup>2-</sup>	<b>0.96</b>	0.14	<b>0.94</b>	-0.44	<b>0.96</b>	1					
Na <sup>+</sup>	<b>1.00</b>	0.22	<b>0.99</b>	-0.32	<b>1.00</b>	<b>0.96</b>	1				
Ca <sup>2+</sup>	<b>0.90</b>	0.06	<b>0.90</b>	-0.35	<b>0.90</b>	<b>0.90</b>	<b>0.89</b>	1			
Mg <sup>2+</sup>	<b>1.00</b>	0.20	<b>0.98</b>	-0.35	<b>1.00</b>	<b>0.97</b>	<b>0.99</b>	<b>0.91</b>	1		
F <sup>-</sup>	-0.19	0.12	-0.19	-0.03	-0.19	-0.23	-0.19	-0.26	-0.22	1	
NO <sub>3</sub> <sup>-</sup>	-0.04	-0.01	-0.07	-0.28	-0.06	-0.08	-0.06	-0.07	-0.07	0.02	1
Cluster 2	WQI	pH	TDS	Alkalinity	Cl <sup>-</sup>	SO <sub>4</sub> <sup>2-</sup>	Na <sup>+</sup>	Ca <sup>2+</sup>	Mg <sup>2+</sup>	F <sup>-</sup>	NO <sub>3</sub> <sup>-</sup>
WQI	1										
pH	-0.30	1									
TDS	<b>0.93</b>	-0.24	1								
Alkalinity	0.33	0.34	0.37	1							
Cl <sup>-</sup>	<b>0.87</b>	-0.50	<b>0.80</b>	0.17	1						
SO <sub>4</sub> <sup>2-</sup>	0.66	-0.37	0.57	0.22	0.66	1					
Na <sup>+</sup>	<b>0.79</b>	-0.15	<b>0.75</b>	0.61	<b>0.72</b>	0.69	1				
Ca <sup>2+</sup>	0.28	-0.14	0.16	0.25	0.40	0.24	0.06	1			
Mg <sup>2+</sup>	<b>0.79</b>	-0.23	<b>0.81</b>	0.51	<b>0.81</b>	0.51	0.65	0.41	1		
F <sup>-</sup>	0.10	0.51	-0.01	0.36	-0.08	-0.05	0.28	-0.26	0.04	1	
NO <sub>3</sub> <sup>-</sup>	0.42	-0.28	0.35	-0.31	0.14	0.09	-0.08	0.05	0.02	-0.27	1

Values in bold indicate strong correlation

in high blood pressure (Grillo et al. 2019). Studies have shown that the utilization of saline groundwater for drinking purposes has led millions of people of Southeast Asia to diseases like hypertension or high blood pressure (Shammi et al. 2019). Further, many types of skin diseases, menstrual problems, miscarriage of pregnancies, acute respiratory infection, and diarrheal diseases have also been found to be associated with the utilization of the saline water for cooking and bathing purposes (Rahaman et al. 2020). The higher concentrations of Ca<sup>2+</sup> and Mg<sup>2+</sup> in the drinking water are also found to be associated with coronary heart disease that increases human mortality (Mora et al. 2017). Additionally, the intake of saline water with high SO<sub>4</sub><sup>2-</sup> concentrations may have laxative effects (Khan et al. 2013). Similarly, the use of a few of the groundwater having higher F<sup>-</sup> and NO<sub>3</sub><sup>-</sup> concentrations for drinking purposes can cause several harmful health effects. The intake of fluoride-enriched groundwater causes mottling of teeth, skeletal fluorosis, osteopenic, osteoporosis, osteo-dental fluorosis, etc. (Farooq et al. 2018). On the other hand, the ingestion of groundwater with high NO<sub>3</sub><sup>-</sup> concentrations leads to methemoglobinemia in infants, gastric cancer, multiple sclerosis, non-Hodgkin lymphoma, and thyroid gland hypertrophy (Chen et al. 2016).

### 3.5 Water Quality for Irrigation Purpose

Wilcox's and United States Soil Laboratory Staff's (USSLS's) diagrams have been utilized to assess the suitability of water for irrigation purposes. The former uses sodium percentage (Na%), while the later uses sodium adsorption ratio (SAR) to classify the water into different categories of irrigation

usage (Richards 1954; Wilcox 1955). Sodium percentage is calculated by dividing the sum of  $\text{Na}^+$  and  $\text{K}^+$  concentrations by total cations (Eq. 5; Raghunath 1987). SAR is calculated as the ratio between  $\text{Na}^+$  and the square root of the average of  $\text{Ca}^{2+}$  and  $\text{Mg}^{2+}$  concentrations (Eq. 6; Richards 1954). For both the calculations, the ion concentrations in meq/L are used.

$$\text{Na}\% = \frac{(\text{Na}^+ + \text{K}^+)}{(\text{Na}^+ + \text{K}^+ + \text{Ca}^{2+} + \text{Mg}^{2+})} \times 100 \quad (5)$$

$$\text{SAR} = \frac{\text{Na}^+}{\sqrt{\frac{(\text{Ca}^{2+} + \text{Mg}^{2+})}{2}}} \quad (6)$$

The collected water samples are distributed in all classes of irrigation, with a majority of samples falling in the unsuitable field of the Wilcox diagram (Fig. 8a). It is observed that around 28% of groundwater and two out of nine surface water samples are excellent to permissible for irrigation, which can readily be utilized for irrigation. About 32% of groundwater and one of the surface water samples belong to permissible to unsuitable category of agricultural usage, and they can be utilized for irrigation in the absence of alternate water sources. The remaining groundwater (40%) and surface water samples (six samples) are found to be unsuitable for irrigation purposes. In view of the cluster classes, it is observed that the samples falling in the unsuitable category of irrigation belong to the C-1 cluster (Fig. 8a). However, 30% of the C-1 samples and all the C-2 samples, including three of the surface water samples, are usable for irrigation purposes. The unsuitability of water for irrigation purposes is caused due to higher Na% and EC values or salinity. The degradation of irrigation water quality due to the increased sodium and salinity hazards has also been seen in others parts of the world (Nematollahi et al. 2016; Brindha et al. 2017; Ismail et al. 2019).

The USSLS's diagram also confirms that the sodium and salinity hazards are responsible for making a majority of water samples unsuitable for irrigation purposes (Fig. 8b). About 74% and 63% of the C-1 samples have very high salinity and sodium hazards, respectively. Long exposure of agricultural soil to saline water causes salinization of the soil, which makes them unusable for agricultural activities (Shrivastava and Kumar 2015). Further, excessive sodium ions in such water are absorbed by the clay particles in the agricultural soil in exchange for  $\text{Ca}^{2+}$  and  $\text{Mg}^{2+}$ , which causes a reduction in soil permeability (Krishnakumar et al. 2014). Around 33% of groundwater and six of the surface water samples are under the influence of very high sodium and salinity hazards; thus, they should not be utilized for irrigation purposes (Fig. 8b). The use of such water for irrigation may damage the soil structure, which in turn affects the water infiltration capacity and permeability of soil (Prasanth et al. 2012). The remaining 67% of groundwater and three of the surface water can be utilized for irrigation purposes. All the C-2 samples belong to these usable classes for irrigation, which is in line with the water sources suitable for drinking purposes. Hence, it is concluded that 67% of the groundwater along with three of the surface water samples are available for irrigational usage in the study area, while a majority of samples grouped in C-1 cluster are unsuitable for irrigation purpose as a result of sodium and salinity hazards.

### 3.6 Spatial Distribution of Water Quality

The spatial variation of WQI can display the distribution of drinking water quality, while variations of SAR and TDS (directly related to EC) can reveal the spatial distribution of



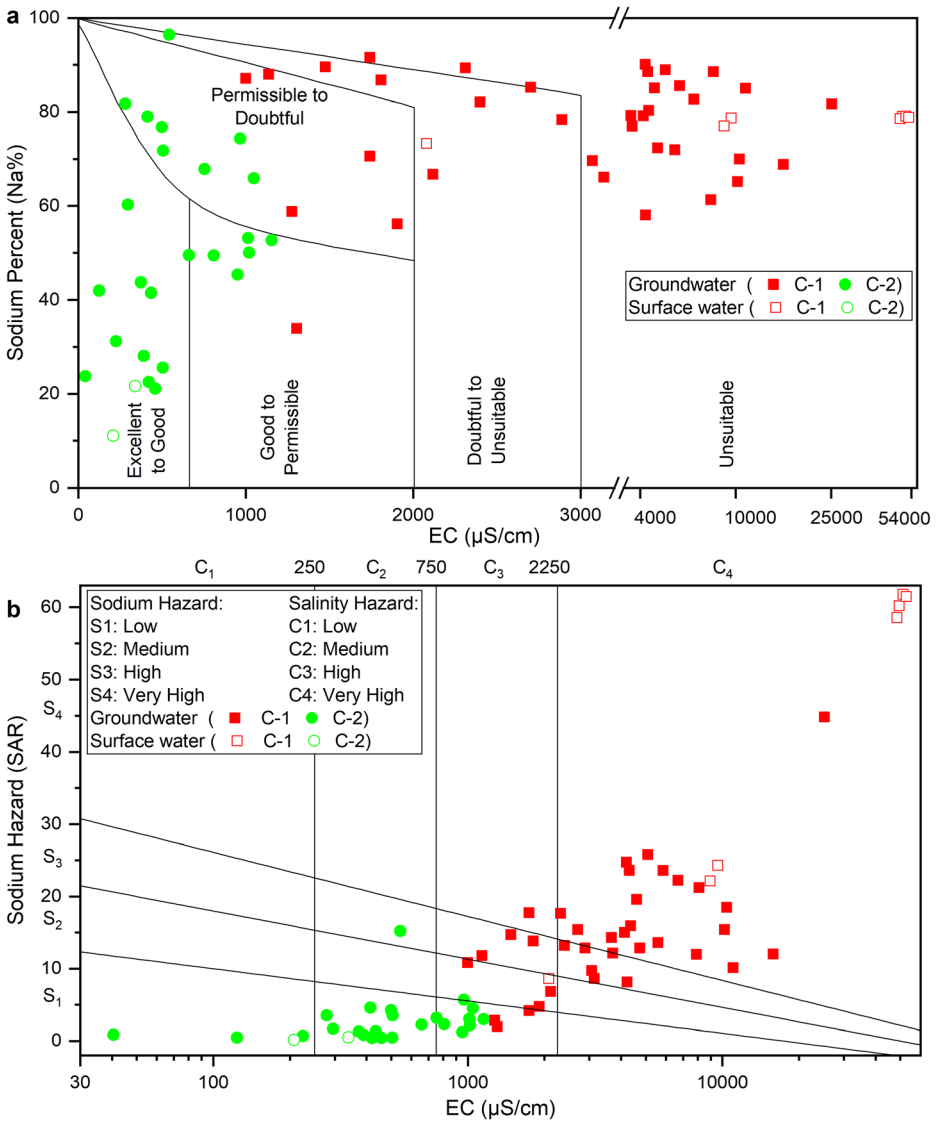


**Fig. 8** Suitability of coastal water for irrigation purpose based on (a) Wilcox's (b) USSLS's diagrams

irrigation water quality in the study area. The spatial variation maps of these parameters were prepared using the spatial analysis module of the geographic information system ArcMap 10.2 (Fig. 9a-c). The surface water samples have extremely higher values and may show anomalous behavior; thus, they were not included in the spatial analysis. The spatial distribution of WQI indicates that the excellent to good water types ( $WQI < 100$ ) occur in small patches, and they occur close to the sea (Fig. 9a). Further, the C-2 sample locations are located above these patches of excellent water types ( $WQI < 50$ ). An earlier study in the study area has reported the occurrence of freshwater patches close to the sea that are associated with the coastal geomorphic features (Prusty et al. 2020). From the spatial distribution of SAR and TDS, it can be observed that the regions up to the second division of SAR ( $< 10$ ) and TDS ( $< 2000$  mg/L) are

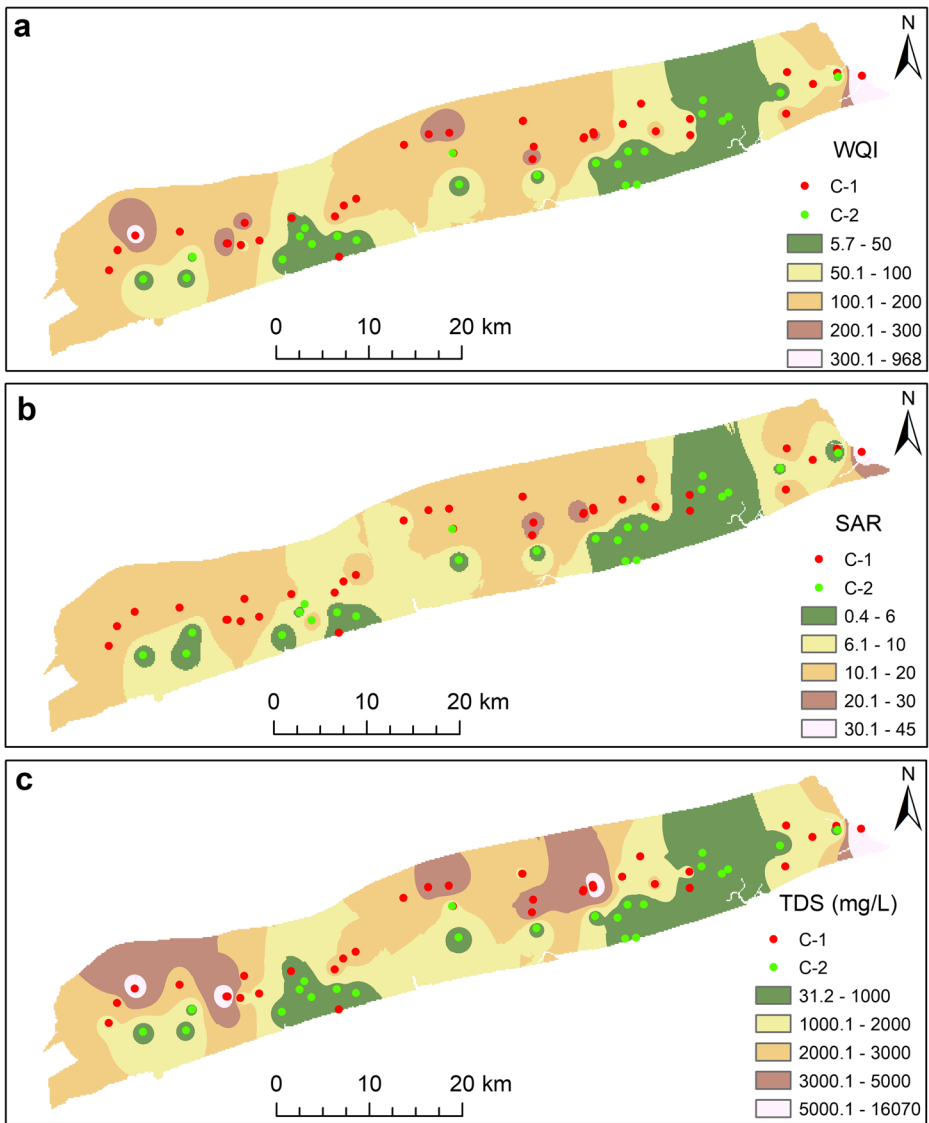


**Fig. 9** Spatial variation of (a) water quality index (WQI), (b) sodium adsorption ratio (SAR), and (c) total dissolved solids (TDS)

suitable for irrigation (Fig. 9b, c). Other regions in the study area have high SAR and TDS values; thus, they are under very high sodium and salinity hazards and cannot be utilized for irrigation purposes. Comparison of spatial variations of WQI, SAR, and TDS indicates that the irrigation water has a slightly higher potential than the drinking water potential in the area. Further, the higher values of WQI and SAR are linked with the higher TDS values or seawater (Fig. 9a-c). The sample locations of the C-1 cluster also mostly occur above these regions. This provides confirmative evidence of the role of seawater in degrading the coastal groundwater quality and making them unsuitable for drinking and irrigation purposes. Thus, the two clusters of water samples show significantly different chemical characteristics and distinct

**Table 4** Characteristics of two clusters of water samples obtained from HCA

Cluster 1 (C-1)	Cluster 2 (C-2)
<ul style="list-style-type: none"> <li>• Comprises 43 water samples (36 groundwater and 7 surface water)</li> <li>• Higher concentrations of water quality parameters</li> <li>• High WQI values and not usable for drinking</li> <li>• Unsuitable for irrigation due to high sodium and salinity hazards</li> <li>• Dominated by Na-Cl water type</li> <li>• Either in the final stage of intrusion or initial stage of freshening</li> <li>• Distributed in inland areas</li> </ul>	<ul style="list-style-type: none"> <li>• Comprises 26 water samples (24 groundwater and 2 surface water)</li> <li>• Lower concentrations of water quality parameters</li> <li>• Low WQI values and suitable for drinking</li> <li>• Usable for irrigation due to low sodium and salinity hazards</li> <li>• Dominated by Na-HCO<sub>3</sub> and Ca-HCO<sub>3</sub> water types</li> <li>• Predominantly in the final stage of freshening</li> <li>• Located in a few patches close to the sea</li> </ul>

spatial distribution patterns in the study area. These characteristics are summarized in Table 4. Utilization of available water resources based on their suitability will help to meet the present water demands. Estimation of the potential of the usable water resources could be helpful in the mitigation of future water demands of the area.

## 4 Conclusions

The study highlights that integrated geochemical, statistical and geospatial analyses can be effectively used to understand the water quality in coastal areas. The influence of seawater on groundwater and surface water has been identified. Geochemical processes such as ion-exchange and sulfate reduction coupled with seawater-freshwater mixing are found to play significant roles in modulating the coastal water chemistry. The hierarchical cluster analysis shows the existence of two clearly defined clusters in the study area. The average cationic dominance is in the order of  $\text{Na}^+ > \text{Mg}^{2+} > \text{Ca}^{2+} > \text{K}^+$  in both clusters, while the average anionic dominance is in the order of  $\text{Cl}^- > \text{SO}_4^{2-} > \text{alkalinity} > \text{NO}_3^- > \text{F}^-$  in the C-1 cluster and  $\text{Cl}^- > \text{alkalinity} > \text{SO}_4^{2-} > \text{NO}_3^- > \text{F}^-$  in the C-2 cluster. The principal component analysis indicates that the samples of the C-1 cluster are characterized by higher salinity, while the samples in the C-2 cluster have lower salinity.

Higher dissolved constituents have led to higher WQI values in 40% of the groundwater samples and all the surface water samples in making them poor to unsuitable for drinking purposes. The presence of sodium and salinity hazards are identified in six of the surface water and 33% of the groundwater samples, which make them unsuitable for irrigation purpose. Under such scenario, tube wells extracting groundwater stands as the only source of drinking water, of which 60% can be utilized for drinking usage. The water sources unsuitable for drinking and irrigation purposes are found to be associated with the seawater influence, while the usable groundwater sources show a patchy distribution in the study area. Periodic monitoring of groundwater and exploration of new potential freshwater sites could help in fulfilling the current and future water demands of the area. Awareness of local communities regarding the appropriate usage of water, based on its quality, may provide an effective tool to manage the coastal water resources.

**Acknowledgements** The authors are thankful to the Ministry of Earth Sciences (MoES), Govt. of India for providing financial support through the Bay of Bengal Coastal Observatory (RP-088). Indian Institute of Technology Bhubaneswar is specially thanked for providing necessary laboratory facilities to carry out this

research work. We express our gratitude to Dr. V. A. Tsihrintzis (Editor-in-Chief), the editorial team, and the anonymous reviewers for their valuable time and encouraging comments in improving the manuscript.

## References

- Adimalla N (2019) Controlling factors and mechanism of groundwater quality variation in semiarid region of South India: an approach of water quality index (WQI) and health risk assessment (HRA). *Environ Geochem Health* 1–28. <https://doi.org/10.1007/s10653-019-00374-8>
- Adimalla N (2020) Assessment and mechanism of fluoride enrichment in groundwater from the hard rock terrain: a multivariate statistical approach. *Geochem Int* 58:456–471. <https://doi.org/10.1134/S0016702920040060>
- Adimalla N, Wu J (2019) Groundwater quality and associated health risks in a semi-arid region of south India: Implication to sustainable groundwater management. *Hum Ecol Risk Assess An Int J* 25:191–216. <https://doi.org/10.1080/10807039.2018.1546550>
- Adimalla N, Li P, Venkatayogi S (2018) Hydrogeochemical evaluation of groundwater quality for drinking and irrigation purposes and integrated interpretation with water quality index studies. *Environ Process* 5:363–383. <https://doi.org/10.1007/s40710-018-0297-4>
- Alfarrah N, Walraevens K (2018) Groundwater overexploitation and seawater intrusion in coastal areas of arid and semi-arid regions. *Water* 10:143. <https://doi.org/10.3390/w10020143>
- Barik SS, Singh RK, Jena PS, Tripathy S, Sharma K, Prusty P (2019) Spatio-temporal variations in ecosystem and CO<sub>2</sub> sequestration in coastal lagoon: A foraminiferal perspective. *Mar Micropaleontol* 147:43–56. <https://doi.org/10.1016/j.marmicro.2019.02.003>
- Brindha K, Neena Vaman KV, Srinivasan K, Sathis Babu M, Elango L (2014) Identification of surface water-groundwater interaction by hydrogeochemical indicators and assessing its suitability for drinking and irrigational purposes in Chennai, Southern India. *Appl Water Sci* 4:159–174. <https://doi.org/10.1007/s13201-013-0138-6>
- Brindha K, Pavelic P, Sotoukee T, Douangsavanh S, Elango L (2017) Geochemical characteristics and groundwater quality in the Vientiane Plain&nbsp;&Laos. *Expo Health* 9:89–104. <https://doi.org/10.1007/s12403-016-0224-8>
- Census of India (2011) CensusInfo India. [http://www.dataforall.org/dashboard/censusinfoindia\\_pca/](http://www.dataforall.org/dashboard/censusinfoindia_pca/). Accessed 8 Aug 2016
- Central Ground Water Board (2013) Groundwater information booklet, Puri District, Orissa. Ministry of Water Resources, Govt. of India. South Eastern Region, Bhubaneswar
- Central Ground Water Board (2014) Report on status of ground water quality in coastal aquifers of India. Ministry of Water Resources, Govt. of India, Faridabad
- Chen J, Wu H, Qian H (2016) Groundwater nitrate contamination and associated health risk for the rural communities in an agricultural area of Ningxia, Northwest China. *Expo Health* 8:349–359. <https://doi.org/10.1007/s12403-016-0208-8>
- Edokpayi JN, Odiyo JO, Durowoju OS (2017) Impact of wastewater on surface water quality in developing countries: A case study of South Africa. In: Tutu H (ed) *Water Quality*. InTech, Croatia, p 428
- Farooq SH, Prusty P, Singh RK, Sen S, Chandrasekharam D (2018) Fluoride contamination of groundwater and its seasonal variability in parts of Purulia district, West Bengal, India. *Arab J Geosci* 11:709. <https://doi.org/10.1007/s12517-018-4062-9>
- Giménez-Forcada E (2010) Dynamic of sea water interface using hydrochemical facies evolution diagram. *Groundwater* 48:212–216. <https://doi.org/10.1111/j.1745-6584.2009.00649.x>
- Giménez-Forcada E (2014) Space/time development of seawater intrusion: A study case in Vinaroz coastal plain (Eastern Spain) using HFE-Diagram, and spatial distribution of hydrochemical facies. *J Hydrol* 517:617–627. <https://doi.org/10.1016/j.jhydrol.2014.05.056>
- Giménez-Forcada E, Sánchez San Román FJ (2015) An excel macro to plot the HFE-diagram to identify sea water intrusion phases. *Groundwater* 53:819–824. <https://doi.org/10.1111/gwat.12280>
- Gopalakrishnan T, Hasan MK, Haque ATMS, Jayasinghe SL, Kumar L (2019) Sustainability of coastal agriculture under climate change. *Sustainability* 11:7200. <https://doi.org/10.3390/su11247200>
- Grillo A, Salvi L, Coruzzi P, Salvi P, Parati G (2019) Sodium intake and hypertension. *Nutrients* 11:1970. <https://doi.org/10.3390/nu11091970>
- Hamed Y, Hadji R, Redhaounia B, Zighmi K, Bâali F, El Gayar A (2018) Climate impact on surface and groundwater in North Africa: a global synthesis of findings and recommendations. *Euro-Mediterranean J Environ Integr* 3:25. <https://doi.org/10.1007/s41207-018-0067-8>

- Horton RK (1965) An index number system for rating water quality. *J Water Pollut Control Fed* 37:300–306
- Ismail AH, Shareef MA, Alatar FM (2019) Hydrochemistry of groundwater and its suitability for drinking and irrigation in Baghdad, Iraq. *Environ Process* 6:543–560. <https://doi.org/10.1007/s40710-019-00374-x>
- Kaiser HF (1974) An index of factorial simplicity. *Psychometrika* 39:31–36. <https://doi.org/10.1007/BF02291575>
- Khan S, Shahnaz M, Jehan N, Rehman S, Shah MT, Din I (2013) Drinking water quality and human health risk in Charsadda district. *Pakistan J Clean Prod* 60:93–101. <https://doi.org/10.1016/j.jclepro.2012.02.016>
- Khatri N, Tyagi S (2015) Influences of natural and anthropogenic factors on surface and groundwater quality in rural and urban areas. *Front Life Sci* 8:23–39. <https://doi.org/10.1080/21553769.2014.933716>
- Krishnakumar P, Lakshumanan C, Kishore VP, Sundararajan M, Santhiya G, Chidambaram S (2014) Assessment of groundwater quality in and around Vedaraniyam, South India. *Environ Earth Sci* 71:2211–2225. <https://doi.org/10.1007/s12665-013-2626-2>
- Kumar PJS, Elango L, James EJ (2014) Assessment of hydrochemistry and groundwater quality in the coastal area of South Chennai, India. *Arab J Geosci* 7:2641–2653. <https://doi.org/10.1007/s12517-013-0940-3>
- Kura N, Ramli M, Sulaiman W, Ibrahim S, Aris A, Mustapha A (2013) Evaluation of Factors Influencing the Groundwater Chemistry in a Small Tropical Island of Malaysia. *Int J Environ Res Public Health* 10:1861–1881. <https://doi.org/10.3390/ijerph10051861>
- Lloyd JW, Heathcote JA (1985) Natural inorganic hydrochemistry in relation to groundwater: an introduction. Clarendon Press, New York
- Mahmuduzzaman M, Ahmed ZU, Nuruzzaman AKM, Ahmed FRS (2014) Causes of Salinity Intrusion in Coastal Belt of Bangladesh. *Int J Plant Res* 2014:8–13. <https://doi.org/10.5923/s.plant.201401.02>
- Matiatos I, Alexopoulos A, Godelitsas A (2014) Multivariate statistical analysis of the hydrogeochemical and isotopic composition of the groundwater resources in northeastern Peloponnesus (Greece). *Sci Total Environ* 476–477:577–590. <https://doi.org/10.1016/j.scitotenv.2014.01.042>
- Milovanovic M (2007) Water quality assessment and determination of pollution sources along the Axios/Vardar River, Southeastern Europe. *Desalination* 213:159–173. <https://doi.org/10.1016/j.desal.2006.06.022>
- Minderhoud PSJ, Erkens G, Pham VH, Bui VT, Erban L, Kooi H, Stouthamer E (2017) Impacts of 25 years of groundwater extraction on subsidence in the Mekong delta, Vietnam. *Environ Res Lett*. <https://doi.org/10.1088/1748-9326/aa7146>
- Mohankumar K, Hariharan V, Rao NP (2016) Heavy Metal Contamination in Groundwater around Industrial Estate vs Residential Areas in Coimbatore, India. *J Clin Diagnostic Res* 10:BC05. <https://doi.org/10.7860/JCDR/2016/15943.7527>
- Mohanty AK, Rao VVSG (2019) Hydrogeochemical, seawater intrusion and oxygen isotope studies on a coastal region in the Puri District of Odisha, India. *CATENA* 172:558–571. <https://doi.org/10.1016/j.catena.2018.09.010>
- Mohapatra PK, Vijay R, Pujari PR, Sundaray SK, Mohanty BP (2011) Determination of processes affecting groundwater quality in the coastal aquifer beneath Puri city, India: a multivariate statistical approach. *Water Sci Technol* 64:809–817. <https://doi.org/10.2166/wst.2011.605>
- Mora A, Mahlknecht J, Rosales-Lagarde L, Hernández-Antonio A (2017) Assessment of major ions and trace elements in groundwater supplied to the Monterrey metropolitan area, Nuevo León, Mexico. *Environ Monit Assess* 189:394. <https://doi.org/10.1007/s10661-017-6096-y>
- Mukhopadhyay R, Karisiddaiah SM (2014) The Indian Coastline: Processes and Landforms. In: Kale VS (ed) *Landscapes and Landforms of India*. Springer, Dordrecht, pp 91–101
- Najib S, Fadili A, Mehdi K, Riss J, Mekan A (2017) Contribution of hydrochemical and geoelectrical approaches to investigate salinization process and seawater intrusion in the coastal aquifers of Chaouia, Morocco. *J Contam Hydrol* 198:24–36. <https://doi.org/10.1016/j.jconhyd.2017.01.003>
- Nematollahi MJ, Ebrahimi P, Ebrahimi M (2016) Evaluating hydrogeochemical processes regulating groundwater quality in an unconfined aquifer. *Environ Process* 3:1021–1043. <https://doi.org/10.1007/s40710-016-0192-9>
- Neumann B, Vafeidis AT, Zimmermann J, Nicholls RJ (2015) Future coastal population growth and exposure to sea-level rise and coastal flooding - A global assessment. *PLoS One* 10:e0118571. <https://doi.org/10.1371/journal.pone.0118571>
- Nguyen TTN, Tran HC, Ho TMH, Burny P, Lebaillly P (2019) Dynamics of farming systems under the context of coastal zone development: The case of Xuan Thuy National Park, Vietnam. *Agriculture* 9:138. <https://doi.org/10.3390/agriculture9070138>
- Patra JP, Mishra A, Singh R, Raghuvanshi NS (2012) Detecting rainfall trends in twentieth century (1871–2006) over Orissa State, India. *Clim Change* 111:801–817. <https://doi.org/10.1007/s10584-011-0215-5>

- Prasanth SVS, Magesh NS, Jitheshlal KV, Chandrasekar N, Gangadhar K (2012) Evaluation of groundwater quality and its suitability for drinking and agricultural use in the coastal stretch of Alappuzha District, Kerala, India. *Appl Water Sci* 2:165–175. <https://doi.org/10.1007/s13201-012-0042-5>
- Prusty P, Farooq SH (2020) Seawater intrusion in the coastal aquifers of India - a review. *HydroResearch* 3:61–74. <https://doi.org/10.1016/j.hydres.2020.06.001>
- Prusty P, Farooq SH, Zimik HV, Barik SS (2018) Assessment of the factors controlling groundwater quality in a coastal aquifer adjacent to the Bay of Bengal, India. *Environ Earth Sci* 77:762. <https://doi.org/10.1007/s12665-018-7943-z>
- Prusty P, Farooq SH, Swain D, Chandrasekharam D (2020) Association of geomorphic features with groundwater quality and freshwater availability in coastal regions. *Int J Environ Sci Technol* 17:3313–3328. <https://doi.org/10.1007/s13762-020-02706-z>
- Rabus R, Hansen TA, Widdel F (2013) Dissimilatory sulfate- and sulfur-reducing prokaryotes. In: Rosenberg E, DeLong EF, Lory S, Stackebrandt E, Thompson F (eds) *The Prokaryotes*. Springer, Berlin Heidelberg, pp 309–404
- Raghunath HM (1987) *Ground Water*, 2nd edn. New Age International, New Delhi
- Rahaman MA, Rahman MM, Nazimuzzaman M (2020) Impact of salinity on infectious disease outbreaks: Experiences from the global coastal region. In: Filho WL, Wall T, Azul AM, Brandli L, Özuyar PG (eds) *Good Health and Well-Being*. Springer, Cham, pp 415–424
- Rezaie AM, Ferreira CM, Rahman MR (2019) Storm surge and sea level rise: Threat to the coastal areas of Bangladesh. In: *Extreme Hydroclimatic Events and Multivariate Hazards in a Changing Environment*. Elsevier, Amsterdam, pp 317–342
- Rice EW, Baird RB, Eaton AD, Clesceri LS (eds) (2012) *Standard methods for the examination of water and wastewater*, 22nd edn. American Public Health Association
- Richards LA (ed) (1954) *Diagnosis and improvement of saline and alkali soils*. US Department of Agriculture, Washington
- Sahu P, Sikdar PK (2008) Hydrochemical framework of the aquifer in and around East Kolkata Wetlands, West Bengal, India. *Environ Geol* 55:823–835. <https://doi.org/10.1007/s00254-007-1034-x>
- Şener Ş, Şener E, Davraz A (2017) Evaluation of water quality using water quality index (WQI) method and GIS in Aksu River (SW-Turkey). *Sci Total Environ* 584–585:131–144. <https://doi.org/10.1016/j.scitotenv.2017.01.102>
- Shammi M, Rahman M, Bondad S, Bodrud-Doza M (2019) Impacts of salinity intrusion in community health: A review of experiences on drinking water sodium from coastal areas of Bangladesh. *Healthcare* 7:50. <https://doi.org/10.3390/healthcare7010050>
- Shrivastava P, Kumar R (2015) Soil salinity: A serious environmental issue and plant growth promoting bacteria as one of the tools for its alleviation. *Saudi J Biol Sci* 22:123–131. <https://doi.org/10.1016/j.sjbs.2014.12.001>
- Subba Rao N, Sunitha B, Adimalla N, Chaudhary M (2020) Quality criteria for groundwater use from a rural part of Wanaparthy District, Telangana State, India, through ionic spatial distribution (ISD), entropy water quality index (EWQI) and principal component analysis (PCA). *Environ Geochem Health* 42:579–599. <https://doi.org/10.1007/s10653-019-00393-5>
- Vijay R, Khobragade P, Mohapatra PK (2011) Assessment of groundwater quality in Puri City, India: an impact of anthropogenic activities. *Environ Monit Assess* 177:409–418. <https://doi.org/10.1007/s10661-010-1643-9>
- Wang X, Zhang J, Gao J, Shahid S, Xia X, Geng Z, Tang L (2018) The new concept of water resources management in China: ensuring water security in changing environment. *Environ Dev Sustain* 20:897–909. <https://doi.org/10.1007/s10668-017-9918-8>
- WHO (2011) *Guidelines for drinking-water quality*, 4th edn. World Health Organization, Geneva
- Wilcox LV (1955) *Classification and use of irrigation waters*. US Department of Agriculture, Washington, DC
- Yidana SM, Yidana A (2010) Assessing water quality using water quality index and multivariate analysis. *Environ Earth Sci* 59:1461–1473. <https://doi.org/10.1007/s12665-009-0132-3>